NASA Technical Memorandum 102044

Results From Baseline Tests of the SPRE I and Comparison With Code Model Predictions

James E. Cairelli and Steven M. Geng
National Aeronautics and Space Administration
Lewis Research Center
Cleveland, Ohio

and

Robert C. Skupinski
Sverdrup Technology, Inc.
NASA Lewis Research Center Group
Cleveland, Ohio

Prepared for the
24th Intersociety Energy Conversion Engineering Conference
cosponsored by the IEEE, AIAA, ANS, ASME, SAE, ACS, and AIChE
Washington, D.C., August 6–11, 1989

NASA

RESULTS FROM BASELINE TESTS OF THE SPRE I AND COMPARISON WITH CODE MODEL PREDICTIONS

James E. Cairelli and Steven M. Geng
National Aeronautics and Space Administration
Lewis Research Center
Cleveland, Ohio 44135

and

Robert C. Skupinski
Sverdrup Technology, Inc.
NASA Lewis Research Center Group
Cleveland, Ohio 44135

ABSTRACT

The Space Power Research Engine (SPRE), a free-piston Stirling engine with linear alternator, is being tested at the NASA Lewis Research Center as part of the Civil Space Technology Initiative (CSTI) as a candidate for high capacity space power. This paper presents results of baseline engine tests at design and off-design operating conditions. The test results are compared with code model predictions.

INTRODUCTION

The work reported in this paper is funded by the NASA Civil Space Technology Initiative (CSTI). Because of its high thermal efficiency potential, Stirling is a candidate for high capacity power for space systems in the late 1990's and into the next century. Since the free-piston Stirling is a relatively immature technology, the SPRE engines were built to serve as research tools to evaluate the engine in its initial form and to provide a test bed for component technology development. This report presents a portion of the test data obtained at the NASA Lewis Research Center with the SPRE I in its original or baseline configuration. Computer predictions using the HFAST code are also presented for comparison.

TEST OBJECTIVES

1. To establish a reference set of data at various operating conditions over a range of temperature ratios from 1.6 to 2.4 and mean pressures from 5.0 to 15.0 MPa. These data are intended for the validation of computer codes and for comparison with future test data.

2. To determine the engine performance sensitivity to variations in operating conditions; particularly its sensitivity to operating temperatures.

3. To check out and tune the facility systems.

SPRE I TEST EQUIPMENT

The SPRE I is one of two engines that were designed and built by Mechanical Technology, Inc., (MTI) of Latham, NY, under contract with NASA. The second engine remains at MTI. These engines were built by splitting the original Space Power Demonstrator Engine (SPDE) in halves and modifying the open hot ends of the cylinders by adding closure heads. References 1 to 3 describe the SPDE program and engine test results. The photograph in Fig. 1 shows the SPRE I installed in the NASA Lewis test facility. Fig. 2 is a cross section drawing of the SPRE showing its major parts. Because of the limited amount of space available in this paper, only the following brief description of the test arrangement is presented.

Heat is supplied to the engine by circulating molten salt through the engine heater. Waste heat is removed from the engine by circulating water through the cooler. Helium is used as the working gas. The engine produces electrical power by means of a linear alternator driven directly by the power piston. The electrical power is absorbed by an electrical resistance load, which controls the alternator output voltage and resulting piston stroke. The SPRE I engine and test facility, including instrumentation, are described in reasonable detail in [4].

GENERAL TEST PROCEDURES

Before starting, the engine was pressurized with helium working gas to 5.0 MPa; the cooling water flow was set to about 1.2 liter/sec; the salt flow was established at about 1.7 liter/sec; and the engine's heater was preheated until the absolute temperature ratio of the heater to cooler metal temperatures was about 1.6. The engine was then started using 60 Hz electrical power. After the engine started, the mean pressure was raised to 7.5 MPa, and data were taken at temperature ratios of 1.7, 1.8, and 2.0. At each temperature ratio data were taken at 5, 6, 7, 8, 9, and 10 mm piston amplitudes (half stroke). While holding the temperature ratio at 2.0, data were also taken at 5.0, 7.5, 10.0, 12.5, and 15.0 MPa for the previously mentioned piston amplitudes. At 15 MPa data were also taken at 10.79 and 11.07 mm (nominal design maximum piston amplitude is 10.0 mm) to determine the actual limit of piston amplitude and output power at 15 MPa and a temperature ratio of

2.0. Data measurements at 15 MPa and at other temperature ratios were planned. However, while preparing to make another test with the engine to complete the data set, the alternator plunger was severely damaged in an unfortunate accident. Considerable time has been required to repair the plunger and to solve a number of other problems. At this writing, engine data have not been measured at 15 MPa for temperature ratios other than 2.0.

CODE PREDICTIONS

The Stirling engine performance code used to generate the predicted data in the plots shown in this report was HFAST, version 1.02. HFAST was written by Mechanical Technology, Inc., (MTI) under MTI internal R&D funding. The major development of HFAST began in 1985 and continued through 1987. The HFAST code is currently being further improved by MTI under contract with NASA. HFAST can simulate both free-piston and kinematic Stirling engines. HFAST assumes that the solution of the governing conservation equations are harmonic functions of time. The solution is then found by solving a system of nonlinear, algebraic equations rather than a system of differential equations.

The SPRE working space was divided into nine control volumes for the computer simulation as shown in Fig. 3. A single control volume was used to model each the displacer appendix gap, expansion space, heater, cooler, and primary compression space. Two control volumes were used to model each the regenerator and the cooler-to-compression-space connecting ducts. This setup neglected the second compression-space volume (see Fig. 2), which exists at the cold end of the displacer. Since HFAST is a one-dimensional code, the addition of the second compression-space volume to the computer model probably would not have had a significant effect on the predictions. When a second compression-space volume was added to the NASA Lewis SPRE code, which is a one-dimensional code, the effect on the code predictions was insignificant.

The actual measured piston and displacer motions, frequencies, mean pressures, salt and water flows, and temperatures were used as inputs to the HFAST code. Predictions were made for compression-space pressure variations, piston PV power, heater and cooler heat flows, piston PV efficiency, and other parameters for comparison to SPRE I measured data.

RESULTS

The initial SPRE I data presented earlier [4] differ from the data presented in this paper. The differences are due to a change in the calculation for the cooler water-side tube wall temperature. After reviewing the range of Prandtl and Reynolds numbers existing in the SPRE cooler, it was determined that the water-side heat-transfer correlation (see [5], Eq. 9.108b) used during the initial testing was not appropriate. The predicted temperature drop between the tube wall temperature and the bulk water temperature tended to be too high. Therefore the calculated cooler wall temperature was higher than the actual cooler wall temperature, and the calculated wall temperature ratio between the heater tubes and the cooler tubes was lower than the actual temperature ratio. The cooler, water-side heat-transfer correlation was replaced with a new correlation [6]. The revised calculation for cooler tube outside-wall temperature has been used for all subsequent tests.

Figure 4 shows the wall temperature ratio determined using the revised calculation versus piston amplitude for the data taken at a wall temperature ratio of 2.0 presented in [4]. For comparison, the calculated wall temperature ratios for the SPRE data reported in this paper are also shown. Although the original data was intended to be at a temperature ratio of 2.0, the temperature ratios were actually higher, approaching 2.1 at 9 mm piston amplitude.

Unless otherwise stated the data plots discussed below are for a temperature ratio of 2.0.

The measured operating frequencies as a function of engine mean pressure at a temperature ratio of 2.0 for 6.0, 8.0, and 10.0 mm piston amplitudes are shown in figure 5. The frequency varies approximately in proportion to the square root of the mean pressure from about 60 to 100 Hz. The frequency is affected slightly by the piston amplitude; tending to drop as piston amplitude increases. At 15 MPa mean pressure the frequency drops 1.4 Hz when the piston amplitude is increased from 6 to 10 mm. This is most likely due to an increase in effective system damping caused by gas flow losses increasing at a higher rate than the power as the piston amplitude is increased.

The piston PV power (rate of work performed on the power piston by the compression-space gas) versus piston amplitude is shown in figure 6. The piston PV power is based on the operating frequency and the integral of P dV using first order harmonic expressions for the compression-space pressure amplitude and phase angle relative to the piston motion, piston amplitude, and piston area. Data are shown for mean pressures of 15.0, 10.0, and 5.0 MPa. The PV power varies nearly linearly with increasing piston amplitude and also with increasing mean pressure raised to about the 1.5 power. The measured power tends to be lower than the predicted power. At 15 MPa the measured power is 6.5 to 8.1 percent lower than the predicted values. The difference between predicted and measured power at 10 MPa tends to increase with piston amplitude from 4.2 to 7.0 percent. At 5 MPa the difference also increases from 6.0 to 9.4 percent as the piston amplitude increases. At 15 MPa and a design maximum piston amplitude of 10 mm, the measured PV power was 11.94 kW, and the predicted power at that condition was 12.99 kW. The maximum PV power achieved by the engine was 12.89 kW at an overstroke piston amplitude of 11.07 mm.

The effect of temperature ratio on PV power is shown in Fig. 7. The PV power at 7.5 MPa mean pressure is plotted against temperature ratio for

piston amplitudes of 10 and 6 mm. The PV power tends to vary nearly linearly with increasing temperature ratio. The code predictions tend to be greater than the measured data by 1.3 to 6.8 percent. The percentage difference increases with increasing temperature ratio and with increasing piston amplitude.

The compression space pressure amplitude versus piston amplitude are shown in Fig. 8. All the measured data falls within about 2 percent of the predicted values.

Figure 9 shows the compression space pressure phase angle versus the piston amplitude. The phase angle was measured with respect to the piston amplitude. The negative sign indicates that the pressure lags the piston motion. The trends in the measured data are similar to the predictions. The pressure phase angle magnitude tends to decrease as the piston amplitude increases, with the slope being greater at 15 MPa. However, the measured phase angles are smaller than the predicted angles (well outside the error bands). The greatest difference is about 0.95° at 5 MPa with 9 mm piston amplitude. The smaller pressure phase angles account for most of the difference between measured and predicted PV power.

The piston PV efficiency versus the piston amplitude is shown in figure 10 for 5 and 15 MPa mean pressure. The PV efficiency was calculated by dividing the piston PV power by the heat flow to the heater. The PV efficiency is relatively insensitive to piston amplitude and mean pressure. The measured values vary only from about 17.5 to 22.6 percent over the full range of piston amplitude and mean pressure. At 5 MPa the efficiency tends to increase as the piston amplitude increases, as predicted. It was 0.37 percentage points higher at 5 mm and tended to fall below the predictions by up to 0.84 points as the piston amplitude increased. The code predicts the efficiency at 15 MPa to be maximum at 5 mm and to decrease as the piston amplitude increases. The measured data at 15 MPa fall below the predictions and tends to peak at about 8 mm. The difference between measured and predicted efficiency at 15 MPa is 2.46 percentage points at 5 mm and decreases to about 1.1 points at 9 and 10 mm.

Figure 11 shows the measured PV efficiency data versus piston PV power for all the data taken at temperature ratio = 2.0. This figure very dramatically shows that the SPRE PV efficiency is nearly constant over more than an order of magnitude range of PV power. The highest PV efficiency occurred at 7.5 MPa over a range of 1.7 to 5.1 kW; varying only from 21.22 to 22.64 percent.

Figure 12 shows the PV efficiency versus temperature ratio at 7.5 MPa for 10 and 6 mm piston amplitude. As expected the PV efficiency increases with temperature ratio. At 10 mm piston/amplitude the measured data are very close (within ±0.5 percentage point) to the predictions. At 6 mm the measured data are 1.64 to 1.05 points higher than the predictions and the difference decreases as the temperature ratio increases.

In Fig. 13 the heat input rate to the heater is shown versus piston amplitude. The measured heat flow varies nearly linearly with piston amplitude and with mean pressure to about the 1.5 power. The measured data generally agrees closely with the predictions. At 15 MPa the measured data ranges from 4.6 percent higher than the prediction at 5 mm to 2.5 percent lower than prediction at 10 mm. At 10 MPa the measured data ranges from 7 to 2.3 percent lower and at 5 MPa the measured data are 8.1 to 5.7 percent lower.

The cooler heat rejection rate is shown in Fig. 14 versus the piston amplitude. The cooler heat flow also varies nearly linearly with piston amplitude and with the mean pressure to about the 1.5 power. At 15 MPa the SPRE data were 0.6 to 2.65 percent lower than predicted. At 10 MPa the measured data ranged from 3.5 percent lower to 0.7 percent higher than the predictions. And at 5 MPa the measured data were 0.4 to 8.9 percent lower than the predicted values.

The expansion space mean gas temperature versus piston amplitude is shown in Fig. 15. The measured temperatures are lower than the predicted temperatures. At 15 MPa the measured temperatures are 0.7 to 7.2° lower than predicted. At 10 MPa the SPRE data were 0.4 to 10.1° lower. And at 5 MPa the measured values were 3.1 to 21.8° lower than predicted. The difference tends to decrease as mean pressure and piston amplitude increase; which suggests possible measurement error due to conduction along the thermocouples or differences between the heat transfer dependent mean value measured by the thermocouples and the time averaged mean gas temperature calculated by the code. Since it was not practical to maintain the salt temperature within small limits while maintaining constant wall temperature ratio, the expansion space temperature variation does not reflect a trend due to the engine but rather the variation in operating conditions.

Figure 16 shows compression space mean gas temperature as a function of piston amplitude. The measured temperatures are lower than the predicted values. At 15 and 10 MPa the measured data are within 2° of the predicted values. At 5 MPa the measured data were lower by 3.7 to 6 °C. The implications of the differences between measured and predicted temperatures are the same as those for the expansion space temperatures.

CONCLUDING REMARKS

The measured data appear to agree fairly well with the HFAST code predictions. The piston PV power agrees within 10 percent and PV efficiency agrees within about 2.5 percentage points. The heat to the heater and heat rejected by the cooler agree within about 9 percent. The trends in measured data generally follow the same trends as the code predictions. The relatively large difference (much larger than the data error band) between measured and predicted compression space pressure phase angle and resulting lower measured PV power and efficiency, as well as the expansion space and compression space temperatures tending always to

be lower than the code predictions suggest possible measurement or measurement interpretation errors and that the code may not accurately represent or recognize some of the losses, heat-transfer, and aerodynamic phenomena associated with oscillating flow. The code also does not account for effects of gas bearing flows and mass transport between volumes of the engine.

The large estimated error bands on PV power and efficiency, heat input and heat rejected are due primarily to the uncertainty in the compression space pressure amplitude and delta temperature measurements for the heater and cooler. Although the engine data suggests that the actual error may be somewhat less than the current estimates, there is a need to improve the accuracy of these measurements through improved setup and calibration or possibly by using alternative techniques with inherently less error.

Further improvement in free-piston Stirling engine performance will depend heavily upon code models to guide hardware design. A major element in the NASA Stirling activities is loss understanding. This effort is being done primarily through contracts and college grants to investigate and model the effects of oscillating flow on viscous losses and heat transfer in the various components of the Stirling cycle as well as losses in gas springs. As they become available, the results of the loss understanding work and experimental engine tests will be integrated into the engine codes.

REFERENCES

[1] G.R. Dochat, "Free-Piston Stirling Engines for Space Power," in Twenty-Second Automotive Technology Development Contractor's Coordination Meeting, Society of Automotive Engineers, Warrendale PA, 1984, pp. 209-213.

[2] J.G. Slaby, "Overview of the 1985 NASA Lewis Research Center SP-100 Free-Piston Stirling Engine Activities," NASA TM-87028, DOE/NASA/1005-5, 1985.

[3] J.G. Slaby, "Overview of Free-Piston Stirling Technology at the NASA Lewis Research Center," NASA TM-87156, DOE/NASA/1005-7, 1985.

[4] J.E. Cairelli, "SPRE I Free-Piston Stirling Engine Testing at NASA Lewis Research Center," NASA TM-100241, 1988.

[5] M.N. Ozisik, Heat Conduction, Wiley, New York, 1980.

[6] S. Whitaker, "Forced Convection Heat Transfer Correlations for Flow in Pipes, Past Flat Plates, Single Cylinders, Single Spheres, and for Flow in Packed Beds and Tube Bundles," AIChE J., vol 18, no. 2, pp. 361-371, Mar. 1972.

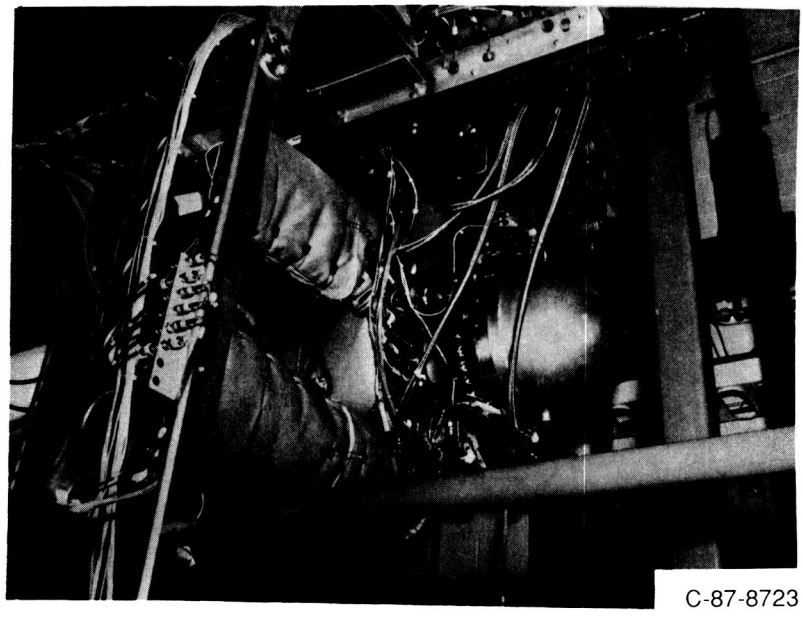

C-87-8723

Fig. 1. - SPRE I installed in the NASA facility.

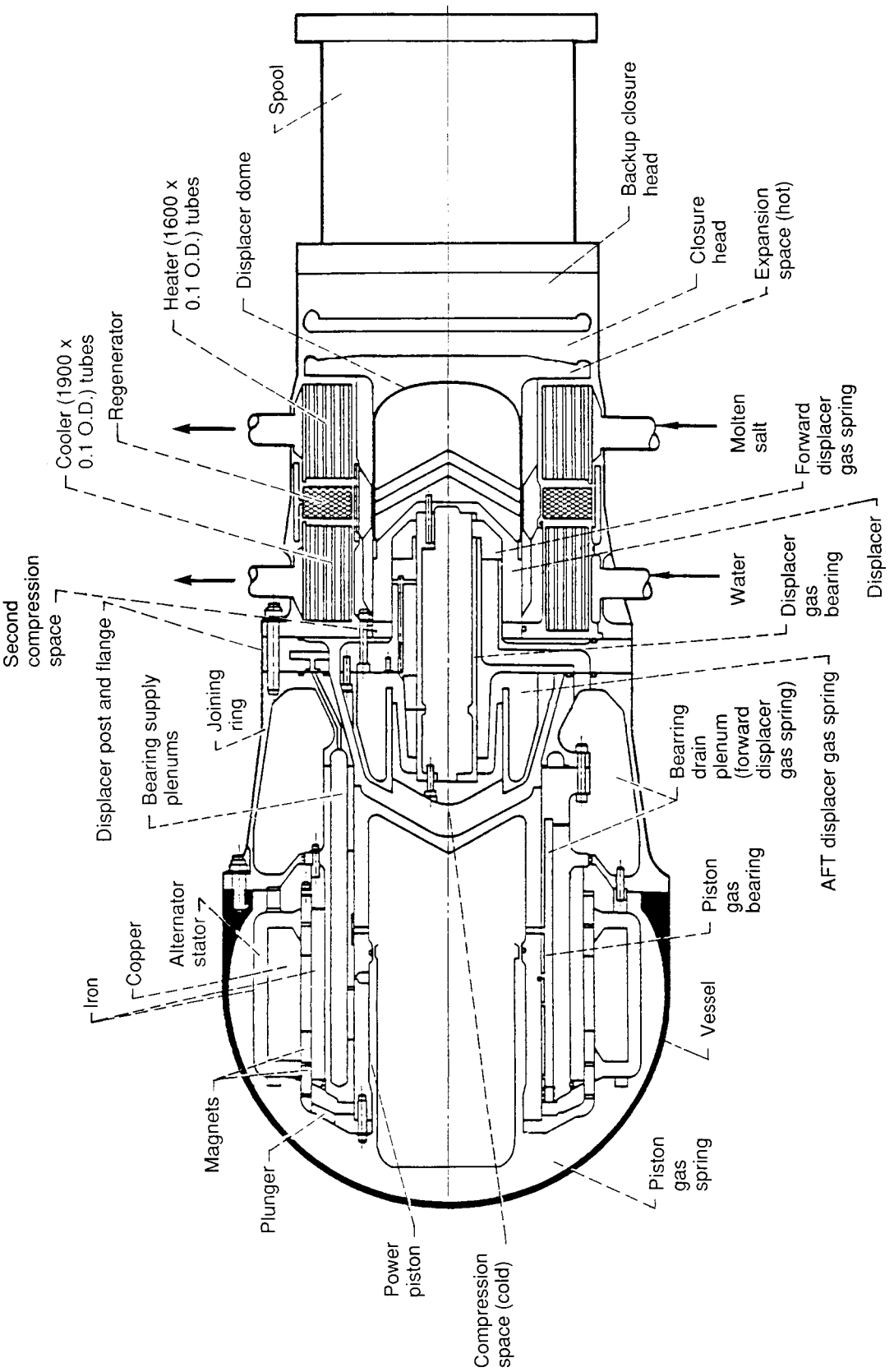

Fig. 2. - SPRE cross section.

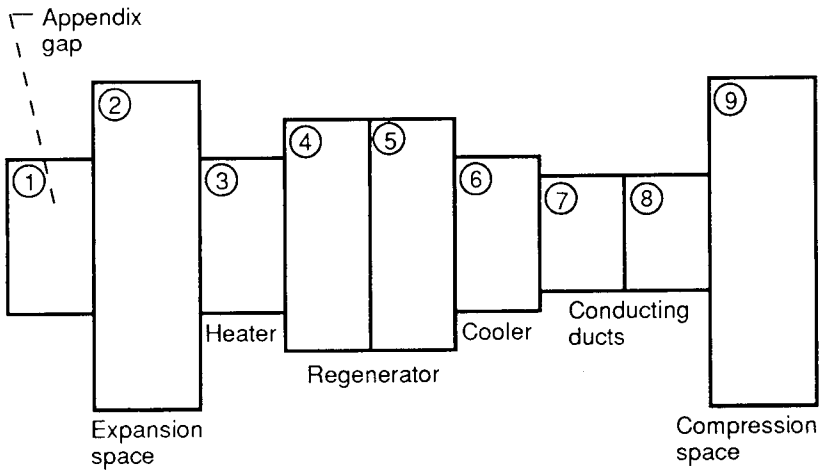

Fig. 3. - Control volumes as a set-up for HFAST computer runs.

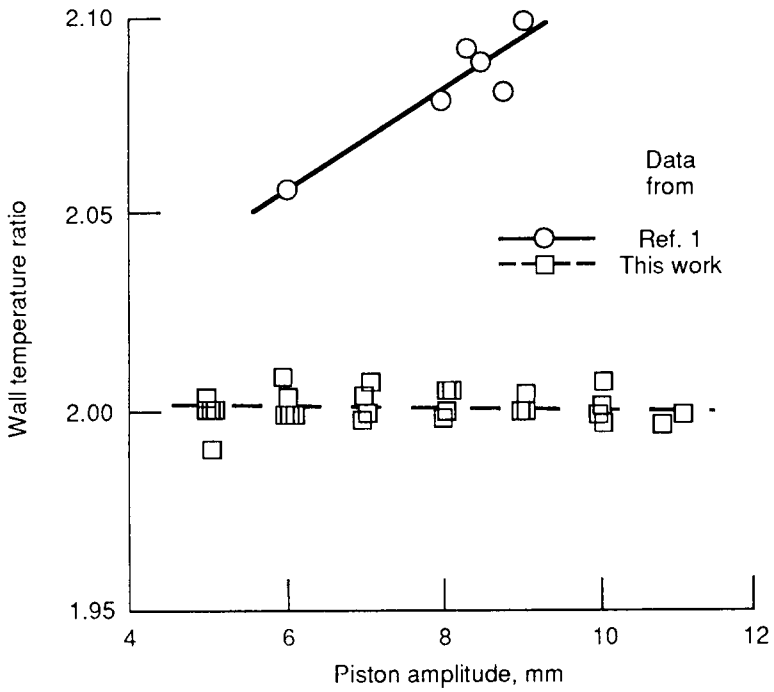

Fig. 4. - Wall temperature ratio versus piston amplitude.

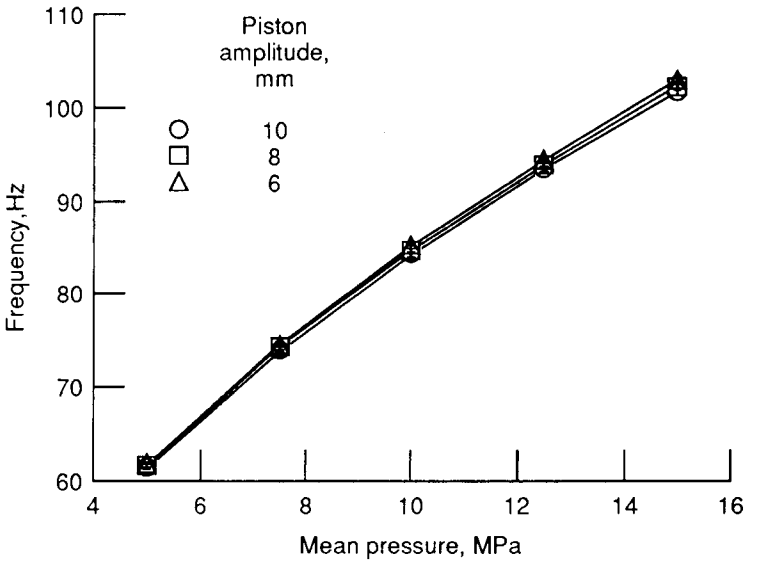

Fig. 5. - Frequency versus mean pressure.

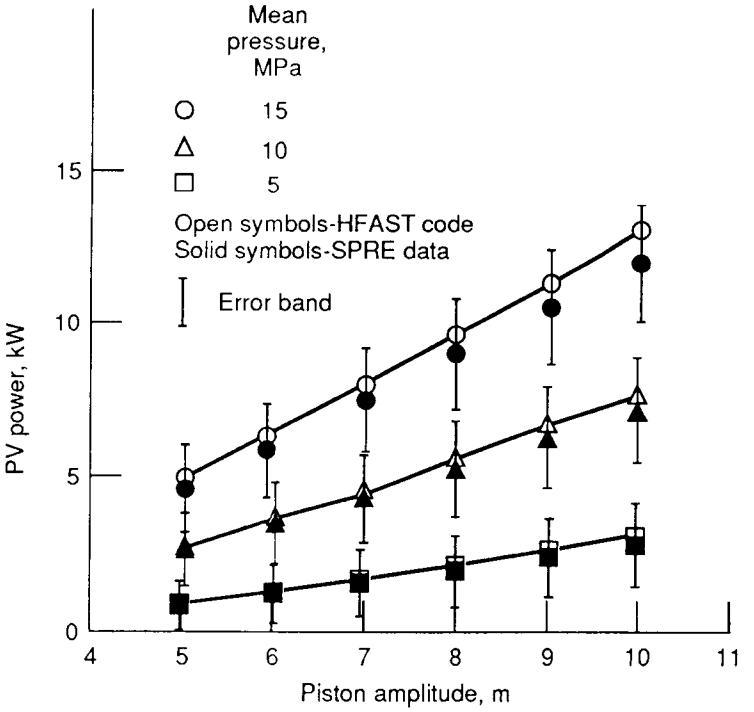

Fig. 6. - Piston PV power versus piston amplitude.

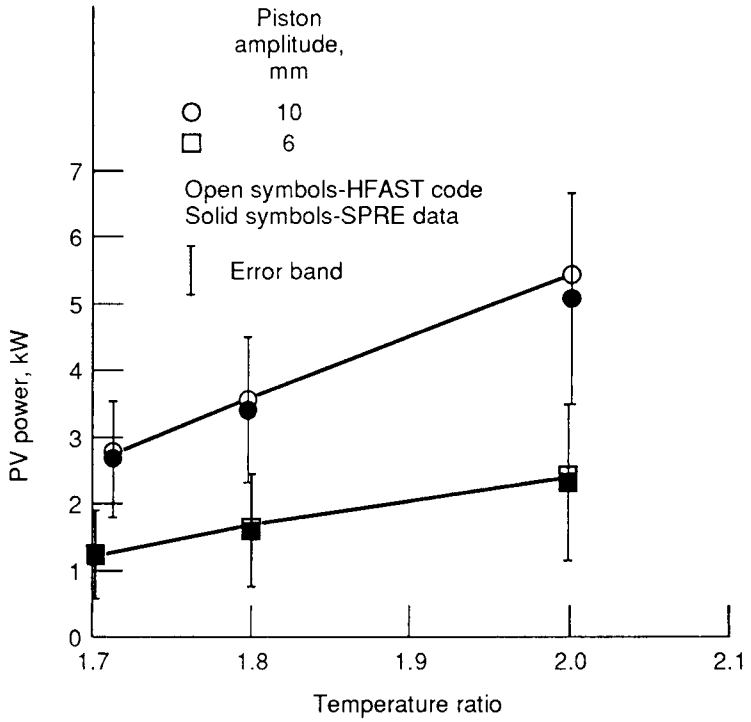

Fig. 7. - Piston PV power versus temperature ratio.

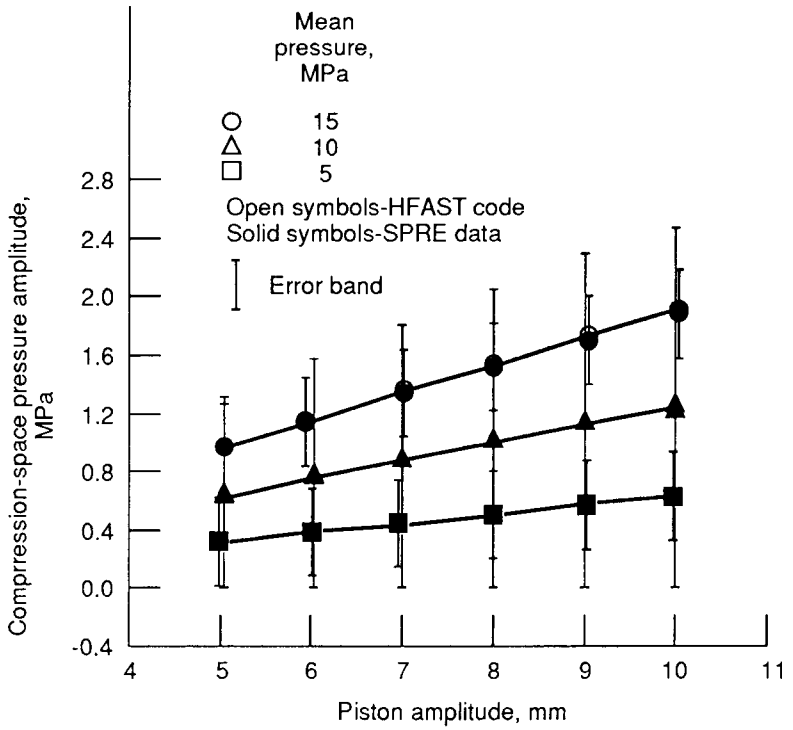

Fig. 8. - Compression-space amplitude versus piston amplitude.

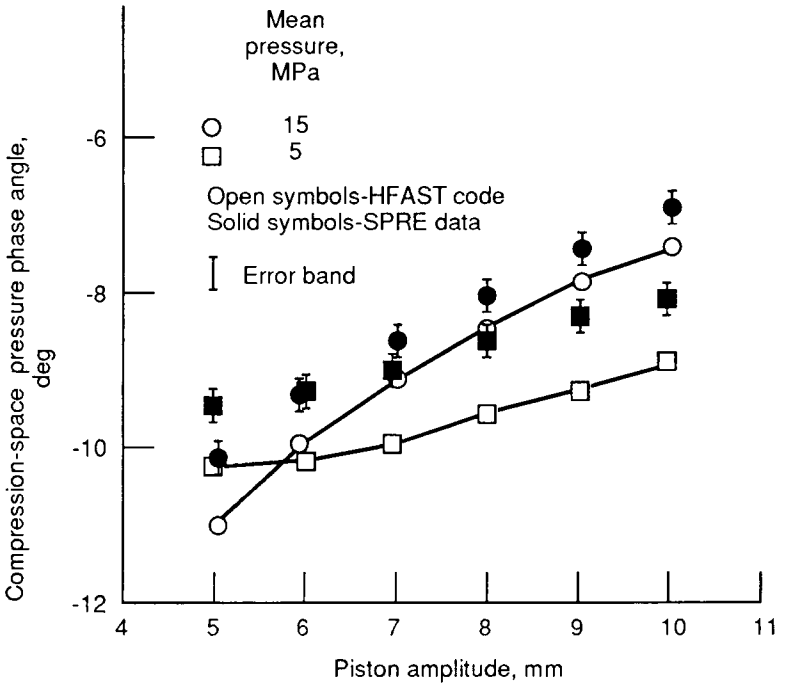

Fig. 9. - Compression-space pressure phase angle versus piston amplitude.

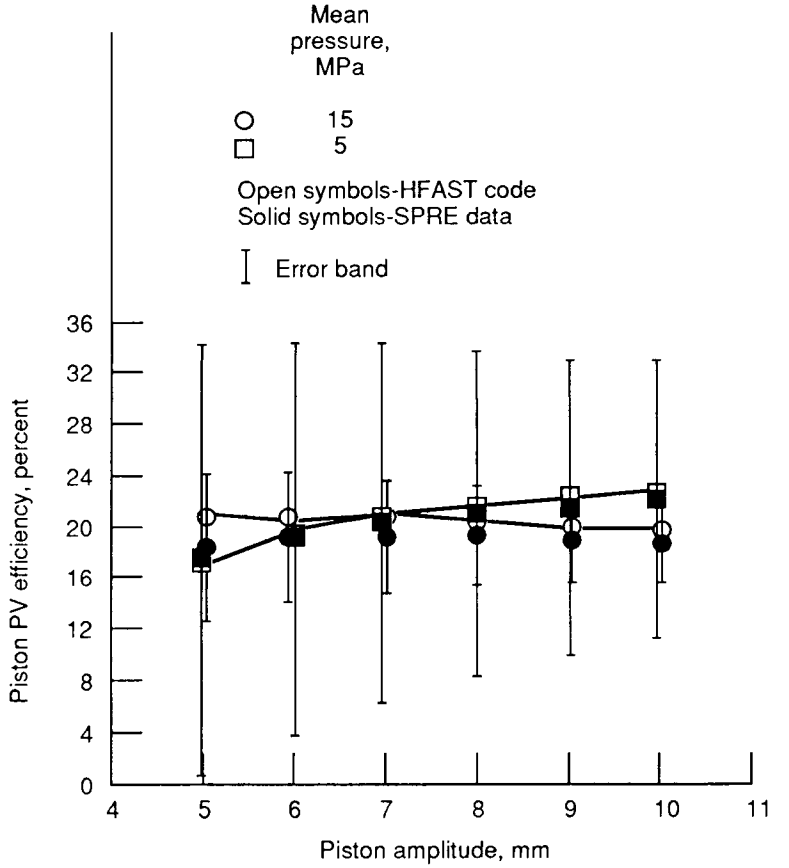

Fig. 10. - Piston PV efficiency versus piston amplitude.

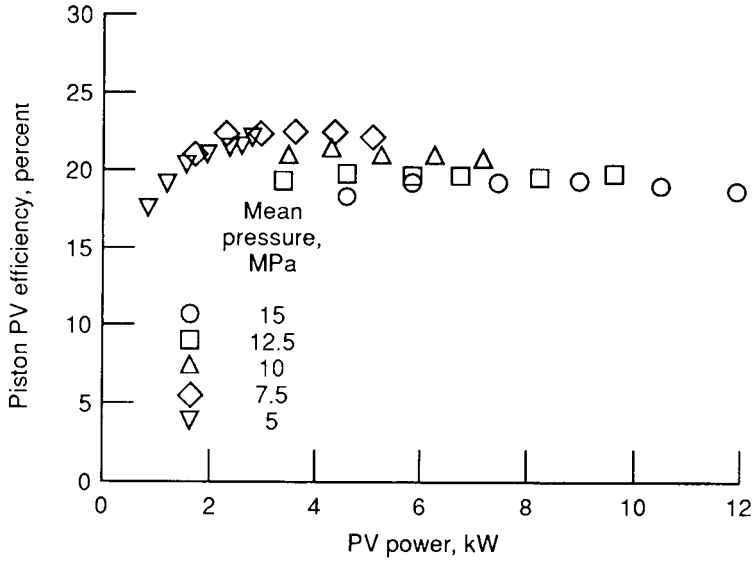

Fig. 11. - Piston PV efficiency versus PV power for SPRE data.

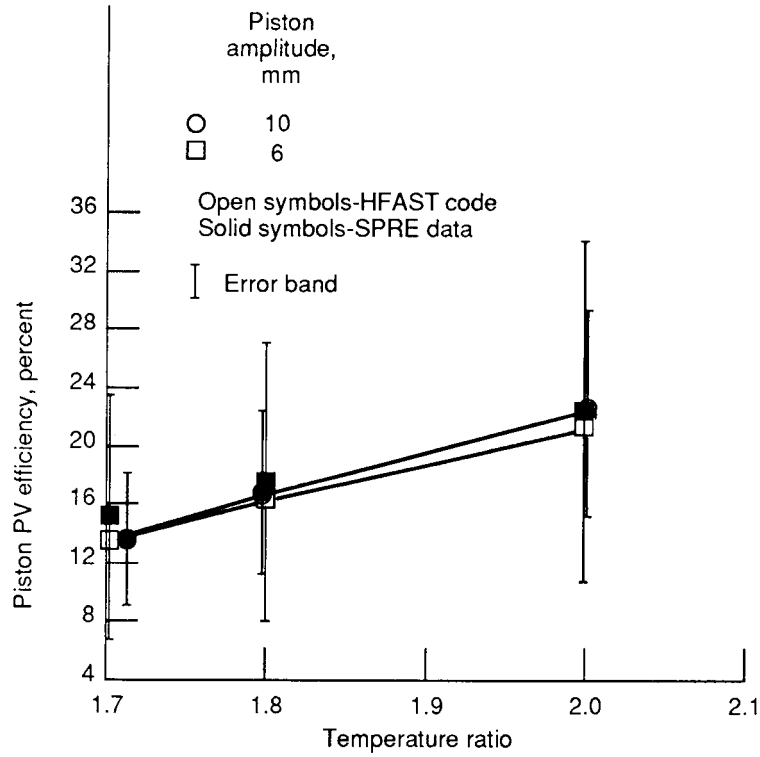

Fig. 12. - Piston PV efficiency versus temperature ratio.

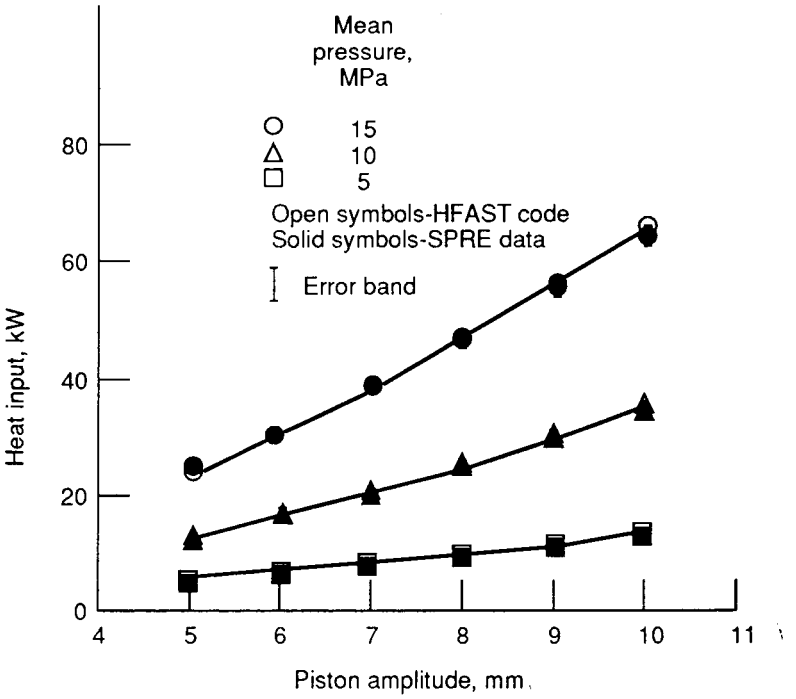

Fig. 13. - Heat input versus piston amplitude.

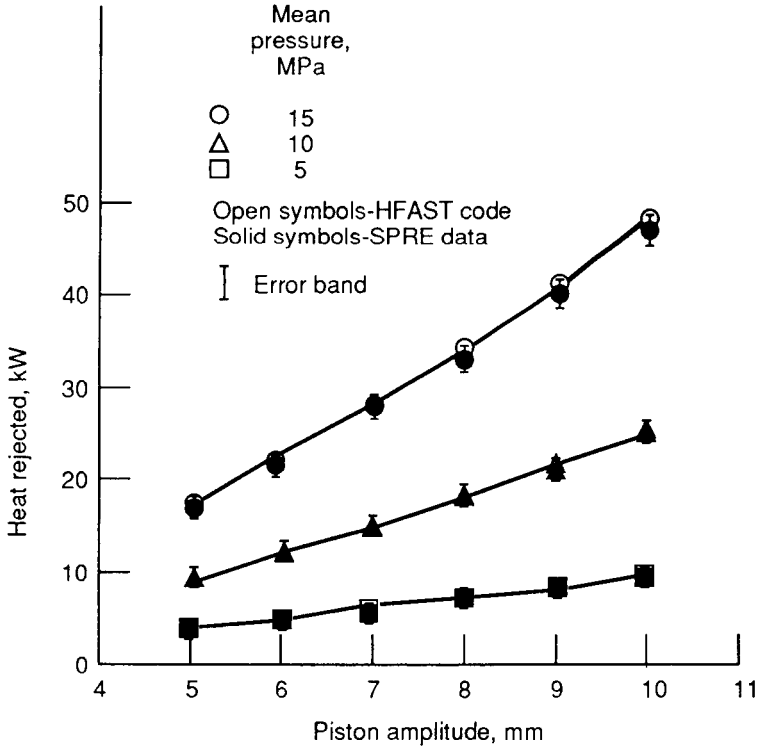

Fig 14. - Heat rejected versus piston amplitude.

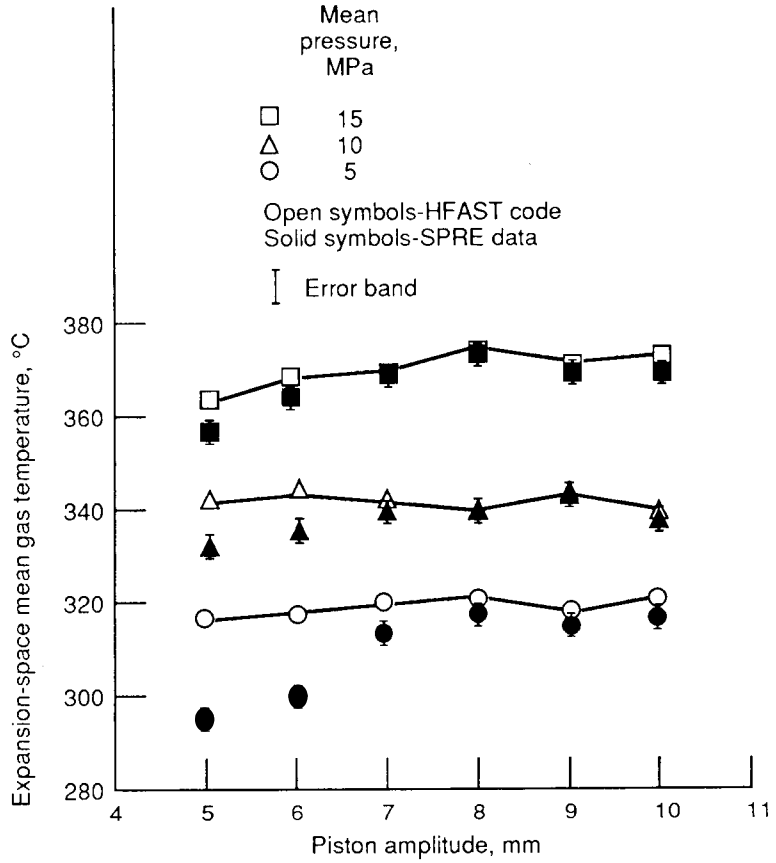

Fig. 15. - Expansion-space mean gas temperature versus piston amplitude.

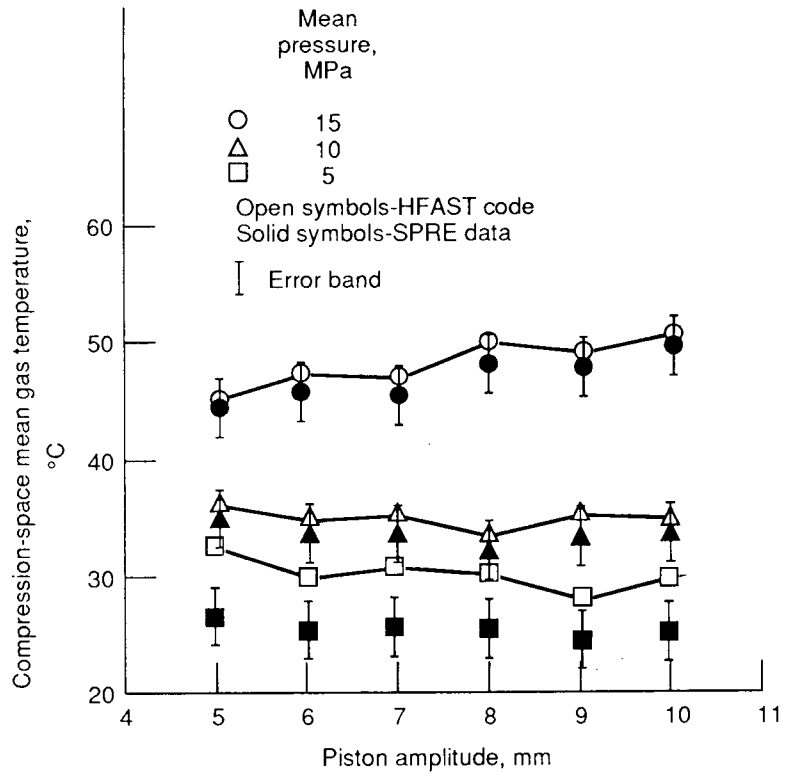

Fig 16. - Compression-space mean gas temperature versus piston amplitude.

NASA
National Aeronautics and Space Administration

Report Documentation Page

1. Report No.	2. Government Accession No.	3. Recipient's Catalog No.
NASA TM-102044		

4. Title and Subtitle	5. Report Date
Results From Baseline Tests of the SPRE I and Comparison With Code Model Predictions	6. Performing Organization Code

7. Author(s)	8. Performing Organization Report No.
James E. Cairelli, Steven M. Geng, and Robert C. Skupinski	E-4792
	10. Work Unit No. 586-01-11

9. Performing Organization Name and Address	11. Contract or Grant No.
National Aeronautics and Space Administration Lewis Research Center Cleveland, Ohio 44135-3191	13. Type of Report and Period Covered Technical Memorandum

12. Sponsoring Agency Name and Address	14. Sponsoring Agency Code
National Aeronautics and Space Administration Washington, D.C. 20546-0001	

15. Supplementary Notes

Prepared for the 24th Intersociety Energy Conversion Engineering Conference cosponsored by the IEEE, AIAA, ANS, ASME, SAE, ACS, and AIChE, Washington, D.C., August 6-11, 1989. James R. Cairelli and Steven M. Geng, NASA Lewis Research Center; Robert C. Skupinski, Sverdrup Technology, Inc., NASA Lewis Research Center Group, Cleveland, Ohio 44135.

16. Abstract

The space power research engine (SPRE), a free-piston Stirling engine with linear alternator, is being tested at the NASA Lewis Research Center as part of the Civil Space Technology Initiative (CSTI) as a candidate for high capacity space power. This paper presents results of baseline engine tests at design and off-design operating conditions. The test results are compared with code model predictions.

17. Key Words (Suggested by Author(s))	18. Distribution Statement
Stirling Free piston Space power experimental data Code predictions	Unclassified - Unlimited Subject Category 20

19. Security Classif. (of this report)	20. Security Classif. (of this page)	21. No of pages	22. Price*
Unclassified	Unclassified	14	A03

NASA FORM 1626 OCT 86

*For sale by the National Technical Information Service, Springfield, Virginia 22161